

Effective viscosity in a wave propagation model for ultrasonic particle sizing in non-dilute suspensions

Raied S. Al-Lashi^{a)}

*Electronics and Computer Science (ECS) Department, Faculty of Physical Sciences and Engineering,
University of Southampton, Hampshire SO17 1B, United Kingdom*

Richard E. Challis

*Electrical Systems and Optics Division, Faculty of Engineering, University of Nottingham, Nottingham NG7 2RD,
United Kingdom*

(Received 3 April 2014; revised 4 August 2014; accepted 8 August 2014)

Estimates of particle size distributions (PSDs) in solid-in-liquid suspensions can be obtained from measurements of ultrasonic wave attenuation. The technique is based on adaptively fitting theoretical wave propagation models to the measured data across a frequency range. These models break down at high solid concentrations and it is believed that this failure is due to the effective viscosity of the mixture in the vicinity of the particles being different from that of the continuous phase. This paper discusses PSD estimation when a number of different viscosity formulations are incorporated into the wave propagation model. The viscosity model due to Happel provides the best estimate of PSD in suspensions of medium concentration. © 2014 Acoustical Society of America.

[<http://dx.doi.org/10.1121/1.4894689>]

PACS number(s): 43.35.Bf, 43.35.Yb [NAG]

Pages: 1583–1590

I. INTRODUCTION

Colloidal materials consist of small particles dispersed in a surrounding liquid with particle sizes in the range 10 nm to 100 μm .¹ A monodisperse mixture contains particles of a single size, and a polydisperse mixture contains a range of particle sizes which is characterized by a particle size distribution (PSD). If the particles are solid the mixture is known as a suspension or slurry, and if they are in the form of liquid droplets the mixture is known as an emulsion. Many commercial materials either exist in colloidal form or pass through a colloidal stage during their manufacture. The PSD is an important measure of product quality because it determines the stability and shelf life, as well as the ultimate functionality of the material. There are frequent requirements to measure PSD for the purposes of process control, quality assurance testing, or basic laboratory investigation. Ultrasonic measurements of attenuation or phase velocity as functions of frequency can be used to estimate PSD and the method is the subject of a number of international standards, such as Ref. 2. They have the advantage over optical techniques that they can be applied to mixtures that are optically opaque.³ The technique has been used by, for example, Davis⁴ to measure mass flow and particle size in coal slurries; McClements and Povey⁵ to examine aqueous sunflower oil emulsions in the context of the food industry, and Holmes *et al.*⁶ to study aqueous suspensions of polystyrene and silica. It is generally recognized that ultrasonic wave attenuation is more sensitive than phase velocity to dispersed particle size,⁵ and so attenuation is the preferred variable for particle sizing.⁷

In the ultrasonic method, the attenuation coefficient is measured as a function of frequency, typically between

1 MHz and a few tens of MHz. A mathematical model is run to simulate the measured attenuation function, see Ref. 8; it has as its inputs the physical properties of the continuous and disperse phases in the mixture and a candidate PSD function. The model is adapted by changing the parameters of the candidate PSD systematically until the best match is obtained between the measured and simulated attenuation functions of frequency. The match is obtained in a least-squared-error sense, typically using the Marquardt algorithm.^{9,10} At this point the adapted candidate PSD is taken to represent the real PSD in the test mixture. The candidate PSD functions are in model form and are typically represented by two parameters—a central size value such as the median, and a width parameter such as standard deviation.

The ultrasonic method breaks down when the concentration of particles is greater than some limit, which can be as low as a few percent by volume. The problem is particularly critical in the case of slurries but less so for emulsions. The first aim of this paper is to investigate the impact of local viscosity in the vicinity of suspended particles on the PSD estimation in high solid concentrations. The second aim is to find the viscosity model that gives the best PSD estimation when using it in the wave propagation model instead of water viscosity. Different viscosity models will be discussed and compared to the measured data. Experimental results for monodisperse and polydisperse slurries will be presented that illustrate these effects and point to the viscosity model that gives the best match to the measured data.

II. VISCOSITY MODELS

In a concentrated slurry the particles are in close proximity—the forces acting on them and their subsequent motions will be affected by surrounding particles, both in flow and in response to an exciting acoustic wave. In the context of the latter, evanescent viscosity waves are thought

^{a)}Author to whom correspondence should be addressed. Electronic mail: R.Al-Lashi@soton.ac.uk

to be generated at the particle surface by mode conversion from an incident compression wave, and these represent energy loss from viscous drag as the particles oscillate to and fro in the acoustic field. In a dilute mixture the viscosity waves merely propagate away from the particle and attenuate rapidly. In a concentrated mixture the viscosity waves from neighboring particles interfere, and this results in changed conditions for the wave-driven oscillation of any given particle. These phenomena have been reviewed in Ref. 1 and later in Ref. 11. The purpose of the current discussion is to extend these earlier works to the problem of PSD estimation in slurries. It is proposed that an effective viscosity model might be found which (1) when incorporated into the wave propagation model gives a reasonable simulation of ultrasonic wave attenuation as a function of frequency and particle concentration, and (2) would provide a practical basis for PSD estimation in slurries. As in earlier work, we invoke an effective viscosity η_{eff} which can be defined as:^{1,12}

$$\eta_{\text{eff}} = Q\eta, \quad (1)$$

where η is the water viscosity and Q is a hydrodynamic correction factor which can be defined as the ratio of the shear force acting on a particle when in a particulate continuum to the force affecting it when it is separated in an infinite continuum of suspending fluid.¹ Q modifies the viscosity in the region of a given particle by including the effects on local viscosity of the surrounding particles in the mixture and the particle shape, which is assumed to be spherical in most analyses.

Viscosity models can be classified as “internal” and “external” flow models.¹³ Internal flow models regard the disperse phase as tubular pores in rigid frames surrounded by the continuous phase. The condition to approximate the suspension as a porous medium is that the length scale of the velocity variations in the fluid must be small in relation to the simple Darcy permeability for the suspension. To satisfy this condition, the shear wavelength in the fluid δ_s is limited by¹

$$\delta_s < \frac{R}{\sqrt{\phi}}, \quad (2)$$

where R is the pore radius and ϕ is the volume fraction occupied by the particles. This corresponds to a limit for volume fraction given by

$$\phi_{\text{max}} = \left[\frac{R}{\delta_s} \right]^2. \quad (3)$$

On the other hand, external flow models consider the fluid moving around suspended particles rather than in hypothetical pores.¹³ We have reviewed both classes of model in Refs. 1 and 11, and so only brief summaries will be given in this paper.

A. Internal flow models

Biot produced a series of papers^{14–17} concerning wave propagation in a porous medium, see also Ref. 1. He derived an effective value of Q as

$$Q = \frac{(1 - \phi)^2}{6\pi RBN}, \quad (4)$$

where N is the number of pores and B is the permeability which is given by the Kozeny-Carman equation as¹⁸

$$B = \left(\frac{R^2}{9k_0} \right) \left[\frac{(1 - \phi)^3}{\phi^2} \right], \quad (5)$$

where k_0 is a free parameter which is related to the tortuosity and the shapes of pores. Thus, Eq. (4) can be expressed as

$$Q = \frac{3k_0\phi^2}{2\pi R^3(1 - \phi)N}. \quad (6)$$

Carman¹⁸ and Hovem^{19,20} discussed the value of k_0 and its relationship to porosity [represented by the term $(1 - \phi)$ in Eq. (6)], shape, and size distribution of the pores. This value will be approximately 5 for spherical and uniform particles, and 10 for elongated particles with different sizes. k_0 would dramatically increase when the porosity exceeds 95%.

B. External flow models

The most basic effective viscosity formula is due to Einstein²¹ and assumes no hydrodynamic interactions between particles; it is

$$Q = (1 + k\phi), \quad (7)$$

where k is a particle shape factor which is 2.5 for rigid spherical particles. It will be clear later that this simple formulation is not adequate for concentrated suspensions.

This was later extended by Vand^{22–24} who allowed temporary agglomerations of particles into doublets, triplets, and so on, to obtain

$$Q = (1 + 2.5\phi + 7.349\phi^2). \quad (8)$$

Hasimoto²⁵ assumed a periodic array of particles in a flow field to obtain

$$Q = \frac{1}{1 - 1.791\phi^{1/2} + \phi - 0.329\phi^2}. \quad (9)$$

The approximation of periodic packing has been further discussed by Zick and Homsy²⁶ and Gibson and Toksoz.²⁷

There are many other approaches that address the viscosity problem in particulate mixtures. A highly relevant group of formulations use the so-called “cell models,” see Strout,²⁸ and Umnova *et al.*¹³ In a cell model, each cell consists of a central particle core surrounded by a spherical cell of fluid which in turn is surrounded by the aqueous mixture of the suspended particles. The overall porosity of the mixture is represented by setting the radius of the surrounding liquid such that:

$$\left(\frac{r}{a} \right)^3 = \phi, \quad (10)$$

where r and a correspond to the radius of the particle and the radius of the fluid shell, respectively. The fluid boundary conditions at the particle surface and the cell surface are key to these models. At the particle surface the radial and tangential stresses are ν_{1r} , ν_{1t} and σ_{1r} , σ_{1t} and at the cell surface are ν_{2r} , ν_{2t} and σ_{2r} , σ_{2t} , with vanishing vorticity at the cell surface. Cell models differ from each other only in the way in which these two sets of boundary conditions are defined physically and treated mathematically. The different treatments have significant effects on the ultrasonic wavenumber.

Kuwabara²⁹ assumed a no-slip condition at the inner boundary whereas the outer boundary combined finite radial velocity (ν_{2r} finite) with zero vorticity. His hydrodynamic correction factor was

$$Q = \frac{5}{5 - 9\phi^{1/2} + 5\phi - \phi^2}. \quad (11)$$

Happel^{30,31} and Happel and Brenner³² considered that the solid particle was coupled to the fluid by a no slip boundary,

as before, while the outer boundary was described by vanishing radial stress, vanishing tangential stress, vanishing radial fluid velocity, and finite tangential velocity ($\nu_{2r}=0$, ν_{2t} finite, $\sigma_{2t}=0$, $\sigma_{2r}=0$), yielding

$$Q = \frac{2 + \frac{4}{3}\phi^{5/3}}{2 - 3\phi^{1/3} + 3\phi^{5/3} - 2\phi^2}. \quad (12)$$

In the models hitherto described Q is independent of frequency whereas in the following two approaches a frequency dependence arises through the shear wavelength in the continuous phase.

Strout²⁸ modified the Happel model by allowing for oscillatory motion of the particle with respect to the cell, obtaining for Q

$$Q_{\text{osc}} = \frac{4}{9}s^2 \left[-i \left(1 - \frac{3}{2}C_1 \right) \right], \quad (13a)$$

where $i = \sqrt{-1}$

$$C_1 = \frac{\begin{bmatrix} S^5 + 3(1 - \phi^{1/3})S^4 + \\ 3(2\phi^{2/3} - 3\phi^{1/3} + 1)S^3 + \\ 3(-2\phi + 6\phi^{2/3} - 3\phi^{1/3})S^2 + \\ 18(\phi^{2/3} - \phi)S - 18\phi \end{bmatrix} + e^{2(1-\phi^{-1/3})S} \begin{bmatrix} S^5 - 3(1 - \phi^{1/3})S^4 + \\ 3(2\phi^{2/3} - 3\phi^{1/3} + 1)S^3 - \\ 3(-2\phi + 6\phi^{2/3} - 3\phi^{1/3})S^2 + \\ 18(\phi^{2/3} - \phi)S - 18\phi \end{bmatrix}}{S^2 D}, \quad (13b)$$

$$D = [(1 - \phi)S^3 + 3(\phi^{4/3} - \phi - \phi^{1/3})S^2 + (9\phi^{4/3} - 3\phi + 6\phi^{2/3})S + (9\phi^{4/3} - 6\phi)] + e^{2(1-\phi^{-1/3})S} [(1 - \phi)S^3 - 3(\phi^{4/3} - \phi - \phi^{1/3})S^2 + (9\phi^{4/3} - 3\phi + 6\phi^{2/3})S - (9\phi^{4/3} - 6\phi)] - e^{2(1-\phi^{-1/3})S} [24\phi S], \quad (13c)$$

$$S = (1 + i)s, \quad (13d)$$

and

$$s = \frac{r}{\delta_s}, \quad (13e)$$

where δ_s is the shear wavelength as defined by Harker and Temple³³

$$\delta_s = (2\eta_{\text{eff}}/\omega\rho_f)^{1/2}. \quad (14)$$

In a dilute system Eq. (13b) simplifies significantly as C_1 becomes

$$C_1 = 1 + \frac{3}{S} + \frac{3}{S^2}. \quad (15)$$

Harker and Temple³³ derived a rigorous expression for Q that incorporated the added or induced mass due to the relative acceleration between the particle and the fluid, the Basset's history term arising from the diffusion of vorticity past the particle and the Stokes drag force. Some re-working of their results leads to the following expression for Q :

$$Q = \frac{i\omega\phi\rho_f Y}{6\pi r\eta N}, \quad (16)$$

where

$$Y = \frac{1}{2} \left(\frac{1 + 2\phi}{1 - \phi} \right) + \frac{9}{4} \cdot \frac{1}{s} + i \frac{9}{4} \left(\frac{1}{s} + \frac{1}{s^2} \right), \quad (17)$$

where s is defined in Eq. (13e). Harker and Temple³³ used the Vand model for viscosity in their calculation of viscous wavelength and subsequently Y . We now compare the impact of using the effective viscosity of the surrounding fluid on the acoustic attenuation and PSD estimation.

III. THE WAVE PROPAGATION MODEL

The calculation of attenuation and PSD is based on a wave propagation model,³⁴ and the one most commonly used is due to Epstein and Carhart³⁵ and Allegra and

Hawley,³⁶ and is known as the ECAH model.² An extension of this model to account for multiple scattering has been formulated by Lloyd and Berry,³⁷ as outlined in Ref. 1. The

original ECAH model was limited to monodisperse mixtures but it can be extended (see Ref. 38) to incorporate J different size bins to get the complex wavenumber β , thus

$$\frac{\beta^2}{k_c^2} = 1 + \sum_{j=1}^J \left[\begin{array}{l} \frac{3\phi_j}{ik_c^3 r_j^3} (A_{0j} + 3A_{1j} + 5A_{2j}) \\ - \frac{27\phi_j^2}{k_c^6 r_j^6} (A_{0j}A_{1j} + 5A_{1j}A_{2j}) \\ - \frac{54\phi_j^2}{k_c^6 r_j^6} \left(A_{1j}^2 + \frac{5}{3}A_{0j}A_{1j} + 3A_{1j}A_{2j} + \frac{115}{21}A_{2j}^2 \right) \end{array} \right]. \quad (18)$$

Here β is the complex wavenumber in the mixture, k_c is the compression wave number in the continuous phase, ϕ_j is the volume fraction of particles of radius r_j , j identifies the size bin, and J is the total number of size bins. A_{0j} , A_{1j} , and A_{2j} are the partial wave amplitude coefficients which pertain to size bin j . On the basis that elemental sinusoids are denoted $e^{+i\omega t}$ the complex wave number is

$$\beta = \frac{\omega}{c(\omega)} - i\alpha(\omega), \quad (19)$$

where ω is angular frequency, $c(\omega)$ is phase velocity, and $\alpha(\omega)$ is the amplitude attenuation coefficient.

As noted earlier, the viscous loss mechanism in the ECAH formulation is associated with evanescent viscosity waves which are generated by mode conversion at the suspended particle boundary. These emanate away from the particle and rapidly disappear in a dilute mixture. In a concentrated mixture the viscosity waves from adjacent particles overlap, and this phenomenon is not included in ECAH, with the result that ECAH tends to over predict attenuation in concentrated slurries. The shear wavelength is always greater than the thermal wavelength which implies that the condition for the close proximity for shear waves will arise at lower particle concentrations than for

thermal waves. The shear wavelength in water at 10 MHz is 1060 nm and for a suspension of 400 nm diameter particles this wavelength corresponds to a limiting particle concentration of only 2.5% v/v. The ECAH model begins to fail when the volume fraction exceeds this concentration limit. Consequently, the ECAH model in its current form cannot be used in estimates of PSD for industrial slurries in which the particle concentration can reach up to, typically, 40% v/v. In Secs. IV and V we will investigate experimentally the potential for an effective viscosity to provide an adequate basis for PSD estimation in non-dilute mixtures.

IV. EXPERIMENTS

The test materials were a polydisperse magnesium hydroxide (Versamag) and a monodisperse aqueous suspension of 30 nm diameter silica spheres (Ludox). Three samples of Versamag with concentrations 2.9%, 4.76%, and 6.54% solid v/v, and 12 samples of Ludox with concentrations in the range 1% to 35% solid v/v were used in the attenuation measurements. The density of Versamag was 2370 kg/m³ (Ref. 39) while the other physical properties were very close to those of silica. Table I gives the physical properties used in subsequent calculations.

TABLE I. Physical parameters used in ECAH simulation.

Parameter (SI units)	Silica (Ludox)	Magnesium hydroxide (Versamag)	Water (25 °C)
c (ms ⁻¹)	5968 ^b	5968 ^b	1497 ^c
ρ (Kgm ⁻³)	2185 ^b	2370 ^b	977 ^c
μ (Nm ⁻²)	3.09e ^{10,b}	3.09e ^{10,b}	
η (Pa s)			8.91e ^{-4,d}
κ (Wm ⁻¹ K ⁻¹)	1.6 ^b	1.6 ^b	0.595 ^d
C_p (J kg ⁻¹ K ⁻¹)	729 ^b	729 ^b	4179 ^b
α/f^2 (Nps ² m ⁻¹)	2.6e ^{-22,a}	2.6e ^{-22,a}	2.3e ^{-14,e}
β_T (K ⁻¹)	1.35e ^{-6,b}	1.35e ^{-6,b}	2.1e ^{-4,b}

^aExperimental measurement.

^bKaye and Laby (Ref. 40).

^cDel Grosso and Mader (Ref. 41).

^dCRC Handbook of Chemistry and Physics.

^eSmith and Beyer (Ref. 42).

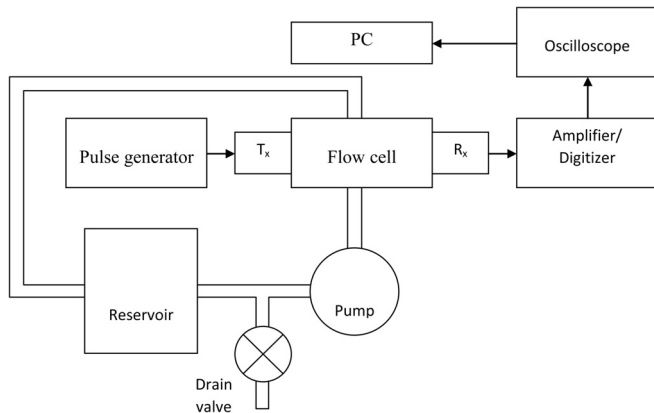


FIG. 1. Schematic representation of the experimental setup. T_x is the transmitting transducer and R_x is the receiving transducer.

Experimental measurements were performed in pitch-catch mode. This approach is based on the transmission of short wide bandwidth ultrasonic compression wave pulses between two thickness mode piezoelectric transducers coaxially aligned in a pumped cell which maintains the particles in suspension. Two pairs of transducers with center frequencies 10 and 25 MHz were used to characterize the slurries. The acoustic path length between the transducers was fixed at 6 mm. Taking the data from the two transducer pairs in combination, the effective frequency bandwidth available for measurement extended from around 5 to 30 MHz. The two sets of data were combined into a single spectrum by fitting a third order polynomial across both sets. The slurry is constantly pumped from the bottom of the reservoir and through the flow cell to prevent the particles from settling at the bottom of the test cell away from the region of the ultrasonic field. Figure 1 shows a block diagram of the system used for attenuation measurement.⁴³

V. APPLICATION OF EFFECTIVE VISCOSITY

In this section we compare the application of various effective viscosity models within ECAH, first in the simulation of ultrasonic attenuation as a function of frequency, and then the combination of ECAH with these viscosities as the basis for PSD estimation.

A. Attenuation

The values of the attenuation at 10 and 30 MHz from experimental data and calculated from ECAH combined with various viscosity models as functions of volume fraction are shown in Figs. 2 and 3, respectively. It can be seen that at higher concentration, and smaller inter-particle distances, the ECAH model with water viscosity overestimates the attenuation, probably due to overlap of the shear fields of neighboring particles. When the alternative viscosity models are used in the ECAH model, the predicted attenuation becomes closer to the measured data, but all the models predict a different attenuation across the concentration range. It can be seen that only the Happel model matches the experimental data but up to approximately 20% v/v at 30 MHz. The Happel model will overestimate the attenuation when

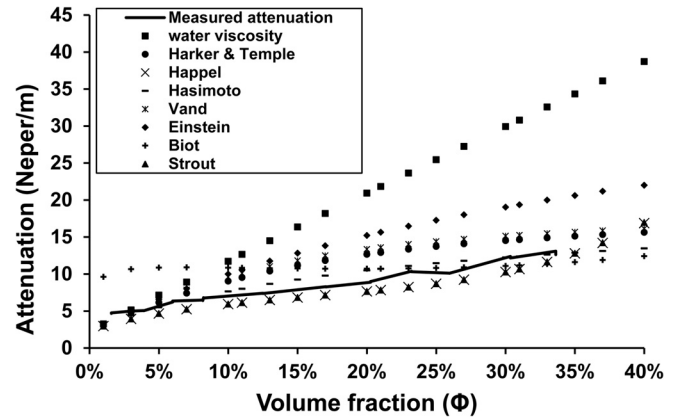


FIG. 2. Measured attenuation at 10 MHz versus volume fraction for the 30 nm diameter silica suspensions (solid line) compared to the predictions of the ECAH model, with various viscosity functions.

the volume fraction exceeds 20% v/v. The predictions of the Strout model match the Happel predicted data across the concentration range. This implies that there is no significant oscillatory motion of the particle in a cell when the size of the particles is small.

B. Particle size distribution

The viscosity models were used with the ECAH model to calculate the mean diameter for a 30 nm aqueous suspension of silica (Ludox) with concentrations in the range 1% and 25.95% v/v as shown in Tables II and III. Overall, the Happel model gives better predictions of the mean than the other models, except at the highest concentration. In order to assess the goodness of fit in the sizing process, a fitting error was calculated by Marquardt algorithm as shown in the fourth column of Tables II and III. The minimum fitting error occurred at the lowest concentration, as would be expected, but also when the viscosity of water was used in the modeling phase of the sizing process; here the predicted mean was lower than that calculated using the other viscosity functions. This implies that the error in the mean results from the formulation for viscosity.

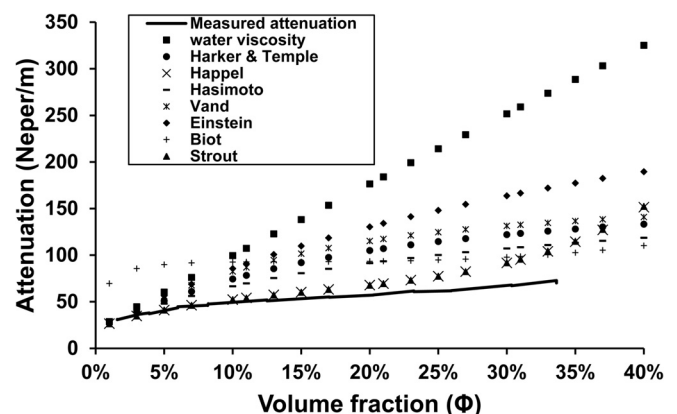


FIG. 3. Measured attenuation at 30 MHz versus volume fraction for the 30 nm diameter silica suspensions (solid line) compared to the predictions of the ECAH model, with various viscosity functions.

TABLE II. Comparison for the estimated mean for 1.5% v/v, 3.25% v/v, and 5.99% v/v aqueous suspensions of 30 nm diameter silica spheres based on using water viscosity and the Vand, Hasimoto, and Happel viscosity models in the fitting process. The density of silica is 2185 kg m^{-3} . The mean corresponds to the particle diameter.

ECAH model	Volume fraction Φ (%)	Mean (μm)	Fitting error (Np^2/m^2)
Water	1.5	26.9	351.3
Vand	1.5	27.4	351.4
Hasimoto	1.5	30.00	352.2
Happel	1.5	33.5	353.4
Water	3.3	23.1	234.4
Vand	3.3	24.0	234.8
Hasimoto	3.3	27.2	236.0
Happel	3.3	31.2	237.9
Water	6.0	19.9	406.3
Vand	6.0	21.5	408.2
Hasimoto	6.0	24.9	412.7
Happel	6.0	29.6	420.5

The PSD estimated by the ultrasonic method was compared to that obtained on the basis of laser light scattering using a *Mastersizer* instrument (Malvern Instruments Ltd., United Kingdom), Figs. 4 and 5. The *Mastersizer* results are less even functions than those obtained ultrasonically; this is because the ultrasonic technique assumes a lognormal form for the PSD and estimates its mean and standard deviation values, whereas the optical method is model-independent. Figure 4 gives the results when the viscosity of water is used in the ECAH fitting process, and here it is clear that, even at the lowest concentration the match to the *Mastersizer* technique is poor, and this worsens as concentration is increased. However, Fig. 5 shows that when the Happel viscosity model is used with ECAH in the fitting process the results show good agreement between the optical and ultrasonic techniques. To further illustrate the effects of viscosity models on

TABLE III. Comparison of the estimated means for 8.22% v/v, 12.36% v/v, 20.62% v/v, and 25.95% v/v aqueous suspensions of 30 nm diameter silica spheres based on using water viscosity and the Vand, Hasimoto, and Happel viscosity models in the fitting process. The density of silica is 2185 kg m^{-3} . The mean corresponds to the particle diameter.

ECAH model	Volume fraction Φ (%)	Mean (μm)	Fitting error (Np^2/m^2)
Water	8.2	18.2	629.1
Vand	8.2	20.2	633.7
Hasimoto	8.2	23.6	642.7
Happel	8.2	28.7	659.7
Water	12.4	15.7	1069.2
Vand	12.4	18.4	1081.6
Hasimoto	12.4	21.6	1099.4
Happel	12.4	26.7	1141.7
Water	20.3	12.9	3910.5
Vand	20.3	16.5	3974.0
Hasimoto	20.3	18.9	4034.4
Happel	20.3	21.9	4242.7
Water	25.9	12.0	8853.5
Vand	25.9	16.3	9001.4
Hasimoto	25.9	18.	9113.8
Happel	25.9	14.9	9586.1

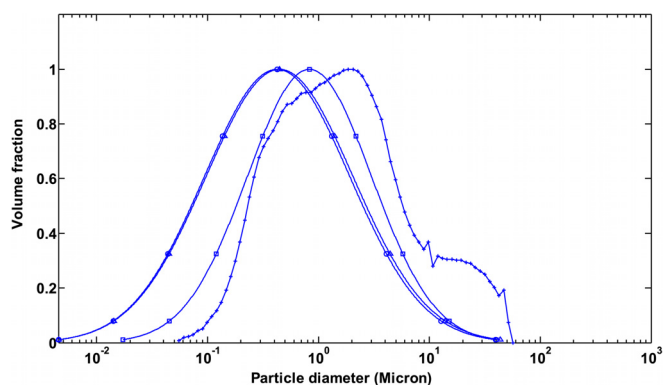


FIG. 4. (Color online) PSD of Versamag estimated ultrasonically and measured by *Mastersizer* instrument (crosses) for three concentrations—2.9% (squares), 4.76% (circles), and 6.54% (triangles). The viscosity of water was used in the ECAH model.

particle size estimation, Table IV shows the median diameter and the standard deviation obtained. The values of the parameters in the *Mastersizer* results were median = $1.8 \mu\text{m}$, standard deviation (sd) = 1.5. The Happel model results in the smallest fitting error in Table IV, and also the PSD properties closest to the *Mastersizer* results. In addition, the values of the median obtained ultrasonically vary considerably between the different viscosity models, although the standard deviations all remained close to the *Mastersizer* result.

It is interesting to observe the quality of fits between the measured and modeled attenuation functions; Fig. 6 compares the attenuation functions fitted on the basis of the viscosity of water, and those derived from the Happel viscosity model, with the measured attenuation. The fits with both viscosities are very close to each other, and reasonably close to the measured data. However, the PSD parameters required to obtain these fits are very different for the two viscosity functions—those for the Happel model better matching the true parameters of the suspension.

VI. DISCUSSION AND CONCLUDING REMARKS

The focus of this paper was the problem of particle sizing in solid-in-liquid suspensions whose concentration was above the dilute limit at which viscosity mediated interaction

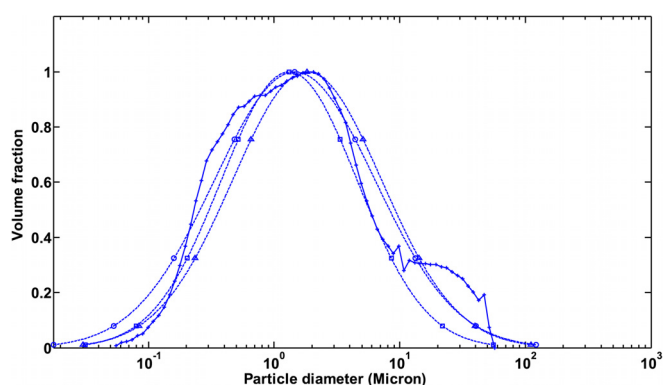


FIG. 5. (Color online) PSD of Versamag estimated ultrasonically and measured by *Mastersizer* instrument (crosses) for three concentrations—2.9% (squares), 4.76% (circles), and 6.54% (triangles). The Happel model for viscosity was used in the ECAH model.

TABLE IV. Comparison of the estimated PSD parameters (median and sd) for a 6.54% v/v aqueous suspension Versamag based on using water viscosity, and the Vand, Hasimoto, and Happel viscosity models in the fitting process. The median corresponds to the particle diameter. The values obtained from the *Mastersizer* were median = 1.8 μm , and sd = 1.5.

ECAH model	Medium (μm)	σ	Fitting error (Np^2/m^2)
Water	0.5	1.5	44 027.5
Vand	0.6	1.5	42 876.6
Hasimoto	1.0	1.6	29 618.9
Happel	1.8	1.4	21 333.5

between particles would compromise the ECAH propagation model as a robust simulator of the ultrasonic attenuation spectrum. For both the magnesium oxide and silica suspensions used in this study this limit was found experimentally to be well below 5% v/v in the tens of MHz frequency range. The essential idea of the work was to take a pragmatic approach to the problem and to investigate the possibility of using existing formulations for an effective viscosity of the mixture, instead of the viscosity of pure continuous phase, as the viscosity input to the ECAH model. This approach has been shown to be successful in that the use of the Happel viscosity model in ECAH provided for successful particle sizing for both of the test materials. The model also provided a good match between measured and simulated ultrasonic attenuation in the case of silica suspensions at concentrations up to around 30% v/v at 10 MHz and 20% v/v at 30 MHz.

Notwithstanding this success, it is to be noted that the Happel model, and others considered in this study, were developed in the context of flow and sedimentation phenomena; they were not aimed at very small scale viscosity phenomena in the vicinity of microscopic particles suspended in a liquid continuum. Thus our approach, although timely in a practical sense, will need further development to place it on a rigorous theoretical basis. In addition, the oscillating particle motions in response to the acoustic wave field are affected by the mass density of the particle as well as the effective viscosity in their local environment. In the current work we have not considered the use of an effective density

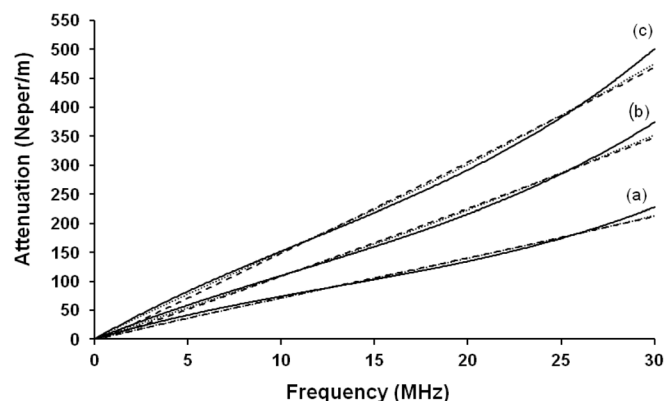


FIG. 6. Fitted attenuation spectra obtained from using water viscosity (broken lines) and Happel viscosity model (dotted lines) in the ECAH model. The solid lines correspond to the measured attenuation spectra. The volume concentrations are: (a) 2.9% v/v, (b) 4.76% v/v, and (c) 6.54% v/v of an aqueous suspension of Versamag.

of the medium surrounding the particles—generally taken as a volume average of the densities of the two phases. The possibility of both effective density and effective viscosity in combination would make a useful future study.

There are two further possibilities for continuing work in this area. Luppé *et al.*⁴⁴ have published work which extends the scattering formulations for wave propagation such as ECAH. For solid-in-liquid suspensions they allow the evanescent viscosity waves from a given particle to re-scatter and mode-convert back to compression waves when they impinge on neighboring particles. This approach better approximates to the physical phenomena which are believed to exist in the micro environment surrounding a suspended particle. It will require some engineering development before it can be applied to particle sizing in an ultrasonic instrument.

The second possibility is based on work by Hipp *et al.*^{45,46} who employed a core-shell scattering model, based on that of Anson and Chivers⁴⁷ as the kernel of a particle sizing algorithm. They demonstrated the success of this approach for suspensions that were well above the dilute limit at which ECAH would begin to fail. However, the core-shell scattering model is computationally complex and prone to ill-conditioning in the inversion of the central 12×12 scattering matrix. In an engineering context, work would be required to stabilize and speed-up the computation before the approach could be used routinely in ultrasonic instruments. For both the Luppé and Hipp approaches, there remains the interesting possibility that they might ultimately be matched to an as yet unknown effective viscosity function which could be incorporated into the standard ECAH model.

We conclude that the effective viscosity approach taken in this work will extend the concentration range for ultrasonic particle sizing in slurries in an engineering context—at least until new scientific developments may supersede it at some future date.

¹R. E. Challis, M. J. W. Povey, M. L. Mather, and A. K. Holmes, "Ultrasound techniques for characterizing colloidal dispersions," *Rep. Prog. Phys.* **68**(7), 1541–1637 (2005).

²BS ISO 20998-1, "Measurement and characterization of particles by acoustic methods—Part 1: Concepts and procedures in ultrasonic attenuation spectroscopy," British Standards Institute, p. 30 (2012).

³A. K. Holmes, R. E. Challis, and D. J. Wedlock, "A wide bandwidth study of ultrasound velocity and attenuation in suspensions: comparison of theory with experimental measurements," *J. Colloid Interface Sci.* **156**(2), 261–268 (1993).

⁴M. C. Davis, "Coal slurry diagnostics by ultrasound transmission," *J. Acoust. Soc. Am.* **64**(2), 406–410 (1978).

⁵D. J. McClements and M. J. W. Povey, "Scattering of ultrasound by emulsions," *J. Phys. D: Appl. Phys.* **22**(1), 38–47 (1989).

⁶A. K. Holmes, R. E. Challis, and D. J. Wedlock, "A wide-bandwidth ultrasonic study of suspensions: the variation of velocity and attenuation with particle size," *J. Colloid Interface Sci.* **168**(2), 339–348 (1994).

⁷A. K. Hipp, G. Storti, and M. Morbidelli, "Particle sizing in colloidal dispersions by ultrasound. Model calibration and sensitivity analysis," *J. Phys. D: Appl. Phys.* **15**(7), 2338–2345 (1999).

⁸S. Meyer, S. Berrut, T. I. J. Goodenough, V. S. Rajendram, V. J. Pinfield, and M. J. W. Povey, "A comparative study of ultrasound and laser light diffraction techniques for particle size determination in dairy beverages," *Meas. Sci. Technol.* **17**(2), 289–297 (2006).

⁹D. W. Marquardt, "An algorithm for least-squares estimation of nonlinear parameters," *J. Soc. Ind. Appl. Math.* **11**(2), 431–441 (1963).

- ¹⁰D. W. Marquardt, "Solution of nonlinear chemical engineering models," *Chem. Eng. Prog.* **55**(6), 65–70 (1959).
- ¹¹R. E. Challis, A. K. Holmes, and V. Pinfield, "Ultrasonic bulk wave propagation in concentrated heterogeneous slurries," in *Ultrasonic Wave Propagation in Non Homogeneous Media*, Springer Proceeding in Physics, edited by A. Léger and M. Deschamps (Springer, Berlin, 2009), Vol. 128, pp. 87–98.
- ¹²M. L. Mather, R. E. Challis, A. K. Holmes, and A. Kalashnikov, "On the problem of the NDE of concentrated slurries," *Rev. Prog. Quant. Nondestr. Eval.*, AIP Conf. Proc. **760**(1), 1266–1272 (2005).
- ¹³O. Umnova, K. Attenborough, and K. M. Li, "Cell model calculations of dynamic drag parameters in packings of spheres," *J. Acoust. Soc. Am.* **107**(6), 3113–3119 (2000).
- ¹⁴M. A. Biot, "Theory of propagation of elastic waves in a fluid-saturated porous solid. I. Low frequency range," *J. Acoust. Soc. Am.* **28**(2), 168–178 (1956a).
- ¹⁵M. A. Biot, "Theory of propagation of elastic waves in a fluid-saturated porous solid. II. Higher frequency range," *J. Acoust. Soc. Am.* **28**(2), 179–191 (1956b).
- ¹⁶M. A. Biot, "Generalized theory of acoustic propagation in porous dissipative media," *J. Acoust. Soc. Am.* **34**(9A), 1254–1264 (1962a).
- ¹⁷M. A. Biot, "Mechanics of deformation and acoustic propagation in porous media," *J. Appl. Phys.* **33**(4), 1482–1498 (1962b).
- ¹⁸P. C. Carman, *Flow of Gases Through Porous Media* (Butterworths, London, 1956), p. 182.
- ¹⁹J. M. Hovem, "Viscous attenuation of sound in suspensions of high-porosity marine sediments," *J. Acoust. Soc. Am.* **67**(5), 1559–1563 (1980a).
- ²⁰J. M. Hovem, "Erratum: Viscous attenuation of sound in suspensions of high-porosity marine sediments," *J. Acoust. Soc. Am.* **68**(5), 1531 (1980b).
- ²¹A. Einstein, "Eine neue Bestimmung der Molekul-dimensionen (A new determination of molecular dimensions)," *Ann. Phys.* **324**(2), 289–306 (1906).
- ²²V. Vand, "Viscosity of solutions and suspensions. I. Theory," *J. Phys. Colloid Chem.* **52**(2), 277–299 (1948a).
- ²³V. Vand, "Viscosity of solutions and suspensions. II. Experimental determination of the viscosity-concentration function of spherical suspensions," *J. Phys. Colloid Chem.* **52**(2), 300–314 (1948b).
- ²⁴V. Vand, "Viscosity of solutions and suspensions. III. Theoretical interpretation of viscosity of sucrose solutions," *J. Phys. Colloid Chem.* **52**(2), 314–321 (1948c).
- ²⁵H. Hasimoto, "On the periodic fundamental solutions of the Stokes equations and their application to viscous flow past a cubic array of spheres," *J. Fluid Mech.* **5**(2), 317–328 (1959).
- ²⁶A. A. Zick and G. M. Homsy, "Stokes flow through periodic arrays of spheres," *J. Fluid Mech.* **115**(1), 13–26 (1982).
- ²⁷R. L. Gibson and M. N. Toksoz, "Viscous attenuation of acoustic waves in suspensions," *J. Acoust. Soc. Am.* **85**(5), 1925–1934 (1989).
- ²⁸T. A. Strout, "Attenuation of sound in high-concentration suspensions: Development and application of an oscillatory cell model," Ph.D. thesis, Department of Chemical Engineering, University of Maine, 1991.
- ²⁹S. Kuwabara, "The forces experienced by randomly distributed parallel circular cylinders or spheres in a viscous flow at small Reynolds numbers," *J. Phys. Soc. Jpn.* **14**(4), 527–532 (1959).
- ³⁰J. Happel, "Viscosity of suspensions of uniform spheres," *J. Appl. Phys.* **28**(11), 1288–1292 (1957).
- ³¹J. Happel, "Viscous flow in multiparticle systems: Slow motion of fluids relative to beds of spherical particles," *AIChE J.* **4**(2), 197–201 (1958).
- ³²J. Happel and H. Brenner, *Low Reynolds Number Hydrodynamics—With Special Applications to Particulate Media* (Prentice Hall, Englewood Cliffs, NJ, 1965), p. 553.
- ³³A. H. Harker and J. A. G. Temple, "Velocity and attenuation of ultrasound in suspensions of particles in fluids," *J. Phys. D: Appl. Phys.* **21**(11), 1576–1588 (1988).
- ³⁴J. S. Tebbutt, "Ultrasonic absorption and phase velocity spectra colloids: Theory, simulation and measurement," Ph.D. thesis, Department of Physics, University of Keele, 1996.
- ³⁵P. S. Epstein and R. R. Carhart, "The absorption of sound in suspensions and emulsions. I. Water fog in air," *J. Acoust. Soc. Am.* **25**(3), 553–565 (1953).
- ³⁶J. R. Allegra and S. A. Hawley, "Attenuation of sound in suspensions and emulsions: Theory and experiments," *J. Acoust. Soc. Am.* **51**(5B), 1545–1564 (1972).
- ³⁷P. Lloyd and M. V. Berry, "Wave propagation through an assembly of spheres. Part I. V. Relations between different scattering theories," *Proc. Phys. Soc.* **91**(3), 678–688 (1967).
- ³⁸R. E. Challis, J. S. Tebbutt, and A. K. Holmes, "Equivalence between three scattering formulations for ultrasonic wave propagation in particulate mixtures," *J. Phys., D: Appl. Phys.* **31**(24), 3481–3497 (1998).
- ³⁹D. R. Lide, *CRC Handbook of Chemistry and Physics: A Ready-Reference Book of Chemical and Physical Data*, 91st ed. (CRC Press, London, 2010), p. 2610.
- ⁴⁰G. W. C. Kaye and T. H. Laby, *Tables of Physical and Chemical Constants*, 16th ed. (Longmans, Harlow, 1995), p. 144.
- ⁴¹V. A. Del Grosso and C. W. Mader, "Speed of sound in pure water," *J. Acoust. Soc. Am.* **52**(5B), 1442–1446 (1972).
- ⁴²M. C. Smith and R. T. Beyer, "Ultrasonic absorption in water in the temperature range 0°–80 °C," *J. Acoust. Soc. Am.* **20**(5), 608–610 (1948).
- ⁴³R. Al-Lashi, "Novel approaches to ultrasonic particle sizing in suspensions with uncertain properties, and to the design of ultrasonic spectrometers," Ph.D. thesis, Electrical and Electronic Engineering Department, University of Nottingham, 2011.
- ⁴⁴F. Luppé, J. Conoir, and A. Norris, "Effective wave numbers for thermo-viscoelastic media containing random configurations of spherical scatterers," *J. Acoust. Soc. Am.* **131**(2), 1113–1120 (2012).
- ⁴⁵A. K. Hipp, G. Storti, and M. Morbidelli, "Acoustic characterization of concentrated suspensions and emulsions. 1. Model analysis," *Langmuir* **18**(2), 391–404 (2002).
- ⁴⁶A. K. Hipp, G. Storti, and M. Morbidelli, "Acoustic characterization of concentrated suspensions and emulsions. 2. Experimental validation," *Langmuir* **18**(2), 405–412 (2002).
- ⁴⁷L. W. Anson and R. C. Chivers, "Ultrasonic scattering from spherical shells including viscous and thermal effects," *J. Acoust. Soc. Am.* **93**, 1687–1699 (1993).